

Six-jet decay of off-shell WW pairs at e^+e^- colliders ¹

Elena Accomando, Alessandro Ballestrero and Ezio Maina

*Dipartimento di Fisica Teorica, Università di Torino
and INFN, Sezione di Torino
v. Giuria 1, 10125 Torino, Italy.*

Abstract

Six-jet events via WW pairs, $e^+e^- \rightarrow W^+W^- \rightarrow q_1\bar{q}_1q_2\bar{q}_2gg$ are studied at tree level using helicity amplitudes. This is the dominant production mechanism for six-jet final states at Lep II energy. ISR effects are taken into account. Total production rates as a function of y_{cut} are given. The relevance of these processes for the issue of colour reconnection is discussed. The cross section for five-jet production via WW pairs at Lep II is also presented.

¹ Work supported in part by Ministero dell' Università e della Ricerca Scientifica.
e-mail: accomando,ballestrero,maina@to.infn.it

Introduction

Several different mechanisms contribute to six-jet production. At Lep II energies they fall into two broad classes: the ‘point-like’ annihilation of e^+e^- to Z^0, γ , which dominates at LEP I energy, and vector boson pair production whose importance grows with increasing energy and dominates above the WW threshold. At still larger energy one should also consider the contribution of three vector bosons. Interference effects between the two set of diagrams are expected to be small since the point-like contribution is dominated by the radiation of four gluons from the two primary quarks with only a small fraction of events with four and possibly six quarks. On the contrary in WW decays there are at least four quarks. Moreover only half of the WW events are flavour neutral and can therefore interfere with the point-like contribution.

In this paper we study the production of off-shell WW pairs and their subsequent decay to five and six jets at e^+e^- colliders. Since $\alpha_s(M_Z) \approx .12$, gluons are radiated with high probability and five- and six-jet fractions are large also at experimentally relevant values of y_{cut} . This mechanism is the main source of five- and six-jet events with total hadronic mass much greater than the mass of the Z . A large number of events with total hadronic mass close to M_Z is produced by radiative return to the Z peak via initial state radiation.

One of the main goals of Lep II is the measurement of the W mass with high accuracy. Fully hadronic decays of the WW pairs represent 4/9 of the cross section. Apart from all the usual uncertainties related to measuring jet energies and directions, which can be partially eliminated by using energy-momentum conservation and possibly the approximate equality of the W^+ and W^- masses, there are uncertainties which stem from the fact that two decays occur in the same event. A jet from, say, the decay of the W^+ can be closer, in a given reconstruction scheme, to a jet from the decay of the W^- than to any other jet from the positively charged W . If the stray jet carries large energy, then the reconstructed masses will be quite far from the W mass which is already at present known with an error of about 200 MeV. One could imagine that such events could be discarded. However, due to the intrinsic width of the W and to all experimental uncertainties, it is impossible to impose very stringent cuts on the difference between the measured mass and the true mass. It is therefore important to estimate the effect of misassigned jets, including the large angle emission tails. For this purpose it is well known that matrix element calculations describe the full angular distribution of jets better than parton shower models while the latter are superior for small angle radiation. It should be mentioned that, due to the number and complexity of the diagrams involved, it is unlikely that a full $\mathcal{O}(\alpha_s^2)$ calculation will be produced in the foreseeable future, and only tree-level matrix elements will be available.

Recently it has been pointed out [1, 2, 3] that cross-talk between the decay of the two W 's can take place also at energy scales much smaller than those typical of jets. This destroys the notion of two separate decays and cast doubts on our ability to reconstruct the masses of the original sources from the decay products, producing potentially large uncertainties. The perturbative contribution to the phenomenon, is related, in the Feynman diagram language, to the presence in the expression for the cross section of interference terms, in which real or virtual partons emitted in the decay of one W are reabsorbed by the decay products of the oppositely charged W . One of

the simplest example is given by the interference between diagrams of type A_1 and diagrams of type A_2 or between diagrams of type A_3 and diagrams of type A_4 in fig. 1.

The contribution of hard gluons, which can be treated perturbatively, to colour rearrangement effects is expected to be small. The argument can be summarized as follows. Only interference terms between different diagrams can produce colour rearrangement; terms in which the gluons emitted by one line are reabsorbed by the same line do not mix the original decays. It is easily realized that all diagrams with a single gluon exchange between the two fermion lines originating from different W 's vanish when the sum over colours is performed. When two, real or virtual, gluons are exchanged, on the contrary non-zero contributions are possible. As a consequence colour rearranged final states are suppressed by α_s^2 compared with normal ones. Moreover, it can be shown that the color factor for the contributions where color rearrangement takes place is smaller by a factor $(N_c^2 - 1)^{-1}$ with respect to the color factor of the leading terms in $1/N_c$ at the same order in α_s . If one compares these terms with the lowest order cross section the ratio of colour factors is $\frac{1}{4} \frac{(N_c^2 - 1)}{N_c^2} = \frac{2}{9}$. A further suppression of the hard gluon contribution to colour reconnection derives from the finite width of the W 's. As an example consider the interference between the diagrams of set A_1 and the diagrams of set A_2 in fig. 1. If the gluons carry a substantial amount of energy at least two of the W propagators must be far off mass shell and therefore the contribution of this term is negligible. The authors of ref. [2] give the following estimate for the ratio between the contribution of colour rearranged diagrams and the total cross section:

$$\frac{\Delta\sigma}{\sigma} \leq \left(\frac{C_F \alpha_s}{N_c} \right)^2 \frac{\Gamma_W}{M_W} \quad (1)$$

In this expression α_s is to be evaluated at $Q^2 = \Gamma_W^2$ where $\alpha_s \approx .25$ so that $\Delta\sigma/\sigma \leq 10^{-3}$.

The non-perturbative contribution to colour reconnection can be described in very simple terms in the string model, arguably the best tool for understanding the fragmentation and hadronization phase of jet development, which links the perturbative gluon cascade to the observed hadrons. In this model, particle production results from the iterative splitting of color strings or antennae which are color singlets and evolve independently of each other. When two color singlet sources, like the two W 's at Lep II, decay close to each other in space-time there two are different ways of forming colour singlets out of the two $q\bar{q}$ pairs. If the primary decays are $W^+ \rightarrow q_1\bar{q}_2$ and $W^- \rightarrow q_3\bar{q}_4$ the $q_1\bar{q}_2$ and $q_3\bar{q}_4$ pairs are always in a relative singlet state. However, with probability $1/9$, the $q_1\bar{q}_4$ and $q_3\bar{q}_2$ pairs can also form colour singlet states. Since the evolution of the antennae is determined by their invariant mass the multiplicity and distribution of detected particles depend strongly on the pairing pattern which is selected.

A more quantitative estimate of color reconnection effects can be obtained using JETSET [4]. In JETSET the primary decay is followed by a perturbative shower evolution, in which successive emissions are strongly ordered in angle as dictated by colour coherence. The showers develop as a Markov-chain process and no colour reconnection takes place in this phase. The two showers expand and when the hadronization phase begins they can overlap. During fragmentation each gluon acts as a $q\bar{q}$ pair and real hadrons are produced by the recursive splitting of colour strings extending between $q\bar{q}$ pairs. It is at this non-perturbative stage that the authors of ref. [2] allow colour

strings to interact, to break and form new strings which may join quark originating from different showers, producing particles which cannot be assigned unambiguously to any of the original W 's. The details of the reconnection mechanism are unknown and require some additional modeling with respect to the well tested basic rules used in JETSET. It is this lack of information in the choice of the reconnection mechanism, that produce the spread in magnitude and even in sign of the predictions for the effects of colour reconnection in the measurement of M_W .

Results

We have studied the reaction $e^+e^- \rightarrow W^+W^- \rightarrow q_1\bar{q}_1q_2\bar{q}_2gg$ at tree level. Six quark final states have not been included since, at e^+e^- colliders, when a pair of gluons is replaced by a quark-antiquark pair, summed over all allowed flavour combinations, the cross section typically decreases by an order of magnitude. Quark masses have been neglected since the contribution of b -quarks is severely suppressed by the smallness of the V_{bc} element of the CKM matrix. The relevant diagrams are shown schematically in fig. 1. For simplicity the lepton part of the diagrams is not drawn and a sum over the three possible structures which describe $e^+e^- \rightarrow WW$ is understood. The set labelled A1 (A2) includes the twenty-four diagrams in which both gluons are emitted in the decay of the W^+ (W^-). Analogously, in A3 we include the twelve diagrams in which one gluon, let us call it g_5 is emitted in the decay of the W^+ while the second, g_6 , is emitted in the decay of the W^- . In A4 the positions of the two gluons are interchanged.

All matrix elements have been computed using the formalism presented in ref. [5] with the help of a set of routines, called PHACT [6], which generate the building blocks of the helicity amplitudes semi-automatically. In our experience this method is faster than others which are commonly used [7, 8, 9]. Further gains in speed can be obtained avoiding subroutine and function calls. In order to achieve this goal the routines in PHACT instead of computing the numerical values of the different terms, write the corresponding FORTRAN code, which can then be compiled and run. In the formalism of [5] it is easy to save every sub-diagram and then to reuse it several times. With this procedure we have generated a rather large piece of code, which however runs quite fast, and therefore can be used in high statistics Montecarlo runs.

The amplitudes have been checked for QCD gauge invariance. We have used $M_Z = 91.1$ GeV, $\Gamma_Z = 2.5$ GeV, $M_W = 80.6$ GeV, $\Gamma_W = 2.06$ GeV, $\sin^2(\theta_W) = .23$, $m_b = 5$. GeV, $\alpha_{em} = 1/128$ and $\alpha_s = .115$ in the numerical part of our work.

Our main results are presented in fig. 2 through 4. Fig. 2a shows the total cross section as a function of y_{cut} in the JADE [10] scheme for the three energies which have been agreed on or are under consideration for Lep II, that is $\sqrt{s} = 175, 190$ and 205 GeV. At such energies the typical value of y_{cut} we have studied, namely $y_{cut} = 5 \times 10^{-3}$ corresponds to a jet-jet invariant mass above 12 GeV. In Fig. 2a initial state radiation (ISR) has been neglected. We see that for a fixed value of y_{cut} the cross section decreases with increasing energy, while, in this range, the WW cross section is increasing. This is due to the definition of y_{cut} :

$$y_{cut} = \frac{2E_i E_j}{s} (1 - \cos \theta_{ij}) \quad (2)$$

which means that at larger center of mass energy larger jet-jet invariant mass are required for an event to pass the cut. On the other hand the mass scale of the decays is obviously given by the W mass and does not change with s . Since small invariant masses are more likely for two jets from the same W than for jets from different W 's one indeed expects the fixed- y_{cut} cross section not to grow as quickly as the cross section for $e^+e^- \rightarrow WW$.

In Fig. 2b we study ISR effects for six-jet production at $\sqrt{s} = 175$ and $\sqrt{s} = 205$. The results at $\sqrt{s} = 190$ have been computed but are not shown for the sake of clarity. We have used the structure function approach at leading-log as in ref. [11]. The cross section is decreased by about 20% at $\sqrt{s} = 175$ and by about 10% at $\sqrt{s} = 205$. The effect at $\sqrt{s} = 190$ nicely interpolates those at the two energies which are shown.

For comparison in Fig. 3 we present the cross sections for five jet production at the same energies used for six jets. We have repeated the calculation of ref. [12] and found complete agreement. The results without ISR are given in fig. 3a and those which compare results with and without ISR effects in fig. 2b. The dot-dashed line in fig. 3a shows the five jet background cross section [13, 14] from $e^+e^- \rightarrow q\bar{q}ggg$ and $e^+e^- \rightarrow q_1\bar{q}_1q_2\bar{q}_2g$.

There is an aspect which deserves some comment. When our results for five-jet production [14] at Lep I are compared with the data presented by ALEPH [15] and OPAL [16] it is clear that the absolute normalization is about a factor of five too small. The simplest explanation for this discrepancy is our choice for α_s . In fact we have used $\alpha_s = .115$ which corresponds to $Q^2 = M_{Z^0}^2$ with $\Lambda_{\overline{MS}} = 200$ MeV with five active flavours in the standard formula:

$$\alpha_s(Q) = \frac{1}{b_0 \log(Q^2/\Lambda^2)} \left[1 - \frac{b_1 \log(\log(Q^2/\Lambda^2))}{b_0^2 \log(Q^2/\Lambda^2)} \right] \quad (3)$$

The analysis of shape variables and jet rates to $\mathcal{O}(\alpha_s^2)$ has shown that, in order to get agreement between the data and the theoretical predictions, the scale of the strong coupling constant has to be chosen to be $Q = x_\mu M_{Z^0}$, with $x_\mu \approx 0.1$ [16]. It has later been shown that when the relevant logarithms are properly resummed [17] agreement is obtained for much larger values of the scale, $x_\mu \approx 1$. [18]. It is therefore not surprising that our tree level expressions require a relatively small scale in order to describe the data. As a consequence the cross sections presented in Fig. 2a,b are expected to be somewhat underestimated. Since α_s is an overall factor our results can be easily modified if a different value for the strong coupling constant is preferred.

Leaving aside the issue of best choice of α_s , with an expected luminosity between 300 and 500 pb^{-1} it is clear that only for $y_{cut} \leq 1.5 \times 10^{-2}$ six jet events can be observed. The cross section grows very rapidly and for $y_{cut} = 5 \times 10^{-3}$ one expects $\mathcal{O}(100)$ decays of a WW pair to six jets per year and per experiment.

In Fig. 4 we present the gluon energy spectrum. The continuous line gives the differential distribution for one fixed gluon, while the dashed line and the short-dash-long-dash line give the energy spectrum for the most and least energetic gluon respectively. These quantities are not directly observable but since in most cases the softest jets are the gluon ones they give an indication of what sort of low energy jets one might expect in WW decays. The softest gluon energy distribution is rather narrow and

peaks at about 8 GeV. The most energetic gluon has a much broader distribution with a maximum at about 20 GeV.

In order to obtain a quantitative estimate of the colour reconnection contribution to the cross section we have integrated over phase space the interference between the diagrams in the set A1 and those in A2 and the interference between the diagrams in the set A3 and those in A4. The interference between (A1+A2) and (A3+A4) is zero. In the following we will call the result σ_{int} . These integrals are particularly challenging. The magnitude and phase of the integrand change rapidly at all W poles and since different sets of particle reconstruct the W mass in different diagrams it is impossible to eliminate the strong peaking structure with the standard change of variable $k_i^2 - M_W^2 = M_W \Gamma_W \tan \theta_i$. In addition the requirement that all jet-jet invariant masses be larger than $M_{min} = sy_{cut}$ introduces discontinuities within the integration region. The accuracy of our results for the interference terms is typically of the order of $1 \div 2\%$, the least accurate point being at $y_{cut} = 1 \times 10^{-3}$ and $\Gamma_W = 2.06$ GeV where the error is about 6.6%. The results presented in fig. 2 through 4 have an accuracy well below 1%.

In the narrow width limit the cross section scales as $(\Gamma_W)^{-2}$ and the bound (1) suggests that the interference terms are proportional to $(\Gamma_W)^{-1}$. Therefore we have investigated the behaviour of σ_{int} as a function of the W width in the range between 10 and 2 GeV. Numerical instabilities become less severe if one artificially increases the W -boson width and this allows us to keep the numerical accuracy of the integration under control. Our results are presented in Fig. 5 for $\sqrt{s} = 175$ GeV and two y_{cut} values, $y_{cut} = 6.5 \times 10^{-3}$ and $y_{cut} = 1 \times 10^{-3}$. For comparison we also plot the curves of the form $y = a/\Gamma_W + b$ which interpolate our results at $\Gamma_W = 10$ GeV and $\Gamma_W = 7$ GeV. In events which do contribute to σ_{int} the gluon energies are restricted from below by the cut on invariant masses and from above by W -width effects as explained previously. The resulting band becomes narrower for increasing y_{cut} and for decreasing Γ_W . This can be clearly seen in Fig. 5. For large values of the W -width the results approximately behave as $a/\Gamma_W + b$ while for values of Γ_W approaching the physical value they gradually fall below the reference curve. This is more evident for $y_{cut} = 6.5 \times 10^{-3}$ where the lower limit of the allowed band is higher. Taking the cross section for $e^+e^- \rightarrow W^+W^- \rightarrow q_1\bar{q}_1q_2\bar{q}_2$ to be 8 pb at $\sqrt{s} = 175$ GeV, $\Delta\sigma/\sigma$ turns out to be 1×10^{-5} at $y_{cut} = 6.5 \times 10^{-3}$ and 5×10^{-4} at $y_{cut} = 1 \times 10^{-3}$, within the bound of ref. [2]. The ratio of the interference terms with the six-jet cross section has a milder dependence on y_{cut} , being 3.3×10^{-4} at $y_{cut} = 6.5 \times 10^{-3}$ and 5.7×10^{-4} at $y_{cut} = 1 \times 10^{-3}$.

Conclusions

We have computed at tree level the cross section for the process $e^+e^- \rightarrow W^+W^- \rightarrow q_1\bar{q}_1q_2\bar{q}_2gg$ which is the dominant contribution to six-jet production at Lep II energies. With a luminosity of 500 pb $^{-1}$ one expects $\mathcal{O}(100)$ decays of a WW pair to six jets per year and per experiment for $y_{cut} = 5 \times 10^{-3}$. We have studied the lowest order non-trivial perturbative contribution to colour reconnection. In the range we have considered, namely $y > 1 \times 10^{-3}$, it is small and within the bound of ref. [2]. We have presented the cross sections for the process $e^+e^- \rightarrow W^+W^- \rightarrow q_1\bar{q}_1q_2\bar{q}_2g$ at Lep II.

References

- [1] G. Gustafson, U. Petterson and P. Zerwas, Phys. Lett. **B209** (1988) 90.
- [2] T. Sjöstrand and V.A. Khoze, Z. Phys. **C 62** (1994) 281.
- [3] G. Gustafson and J. Häkkinen, Z. Phys. **C 64** (1994) 659.
- [4] T. Sjöstrand, Comput. Phys. Commun. **39** (1986) 347; T. Sjöstrand and M. Bengtsson, Comput. Phys. Commun. **43** (1987) 367.
- [5] A. Ballestrero and E. Maina, Phys. Lett. **B350** (1995) 225.
- [6] A. Ballestrero, in preparation.
- [7] R. Kleiss and W.J. Stirling, Nucl. Phys. **B262** (1985) 235.
- [8] C. Mana and M. Martinez, Nucl. Phys. **B287** (1987) 601.
- [9] K. Hagiwara and D. Zeppenfeld, Nucl. Phys. **B274** (1986) 1.
- [10] JADE Collaboration, W. Bartel *et al.*, Z. Phys. **C 33** (1986) 23.
JADE Collaboration, S. Bethke *et al.*, Phys. Lett. **B213** (1988) 235.
- [11] G. Montagna, O. Nicosini, G. Passarino and F. Piccinini, Phys. Lett. **B348** (1995) 178.
- [12] N. Brown, Z. Phys. **C 51** (1991) 107.
- [13] N.K. Falck, D. Graudenz and G. Kramer, Nucl. Phys. **B328** (1989) 317.
- [14] A. Ballestrero and E. Maina, Phys. Lett. **B323** (1994) 53.
- [15] L3 Collaboration, B. Adeva *et al.*, Z. Phys. **C 55** (1992) 39.
ALEPH Collaboration, D. Buskulic *et al.*, Z. Phys. **C 55** (1992) 209.
- [16] DELPHI Collaboration, P. Abreu *et al.*, Z. Phys. **C 54** (1992) 55.
OPAL Collaboration, P.D. Acton *et al.*, Z. Phys. **C 55** (1992) 1.
- [17] S. Catani, L. Trentadue, G. Turnock and B.R. Webber, Phys. Lett. **B263** (1991) 491.
S. Catani, L. Trentadue, G. Turnock and B.R. Webber, Nucl. Phys. **B407** (1983) 3.
S. Catani, G. Turnock and B.R. Webber, Phys. Lett. **B272** (1991) 368.
S. Catani, G. Turnock and B.R. Webber, Phys. Lett. **B295** (1992) 269.
G. Turnock, Cambridge Preprint Cavendish-HEP-92/3; Ph.D. Thesis, U. of Cambridge (1992).
J.C. Collins and D.E. Soper, Nucl. Phys. **B193** (1981) 381.
J.C. Collins and D.E. Soper, Nucl. Phys. **B197** (1982) 446, Err. Nucl. Phys. **B213**

(1983) 545.

J.C. Collins and D.E. Soper, Nucl. Phys. **B284** (1987) 253.

J. Kodaira and L. Trentadue, Phys. Lett. **B112** (1982) 66.

R. Fiore, A. Quartarolo and L. Trentadue, Phys. Lett. **B294** (1992) 431.

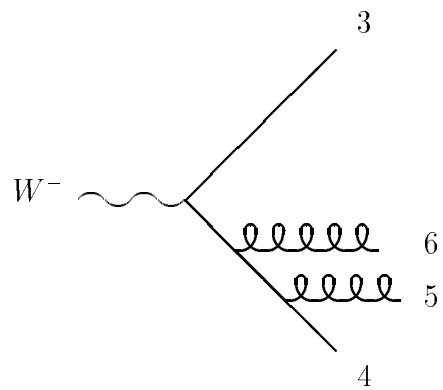
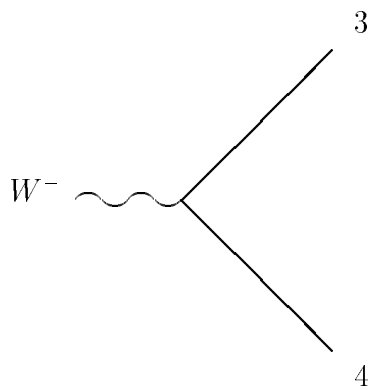
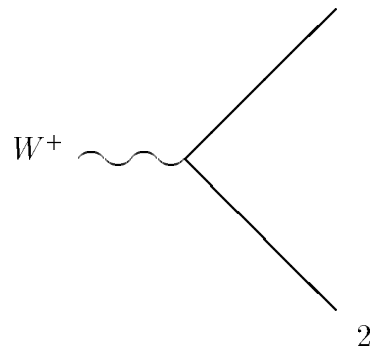
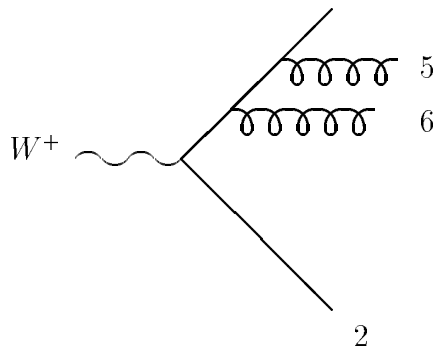
S. Catani, Yu.L. Dokshitzer, M. Olsson, G. Turnock and B.R. Webber, Phys. Lett. **B269** (1991) 432.

S. Catani, Yu.L. Dokshitzer, F. Fiorani and B.R. Webber, Nucl. Phys. **B377** (1992) 445.

- [18] OPAL Collaboration, P.D. Acton *et al.*, Preprint CERN-PPE/93-38, March 1993.
DELPHI Collaboration, P. Abreu *et al.*, Preprint CERN-PPE/93-43, March 1993.

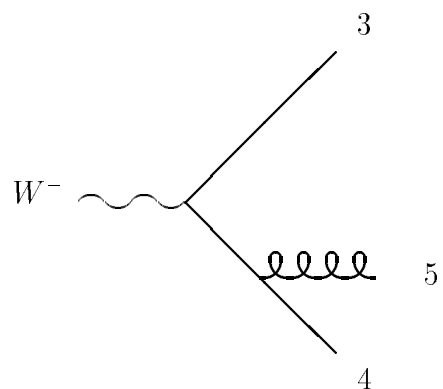
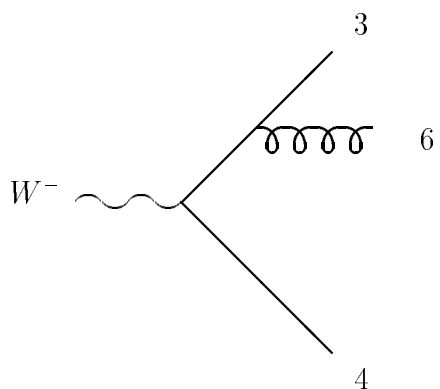
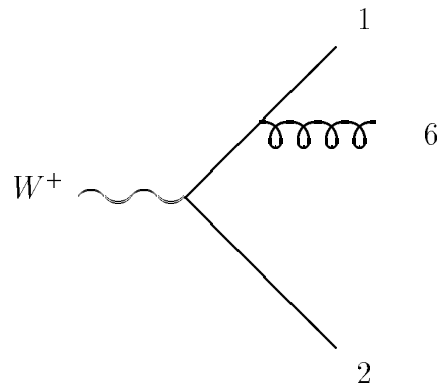
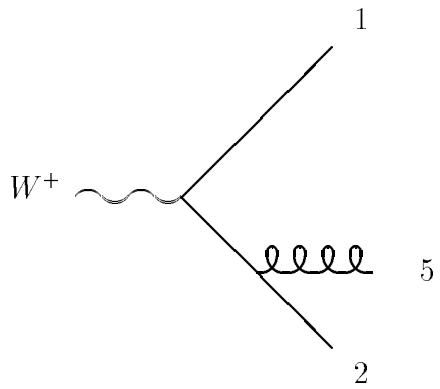
Figure Captions

- Fig. 1** Representative diagrams of the decay part contributing to $e^+e^- \rightarrow WW \rightarrow q_1\bar{q}_2q_3\bar{q}_4gg$. For simplicity the lepton part of the diagrams is not drawn and a sum over the three possible structures which describe $e^+e^- \rightarrow WW$ is understood. In set A1 (A2) we include the eight diagrams in which both gluons are emitted in the decay of the W^+ (W^-). Analogously in set A3 we include the four diagrams in which gluon g_5 is emitted in the decay of the W^+ while g_6 is emitted in the decay of the W^- . In A4 the positions of the two gluons are interchanged.
- Fig. 2** Total cross section as a function of y_{cut} in the JADE scheme for six-jet production via WW at $\sqrt{s} = 175$ GeV (continuous line), $\sqrt{s} = 190$ GeV (dashed line) and $\sqrt{s} = 205$ GeV (dotted line). In Fig. 2a ISR effects are not included. In Fig. 2b we compare results which include ISR effects with those without ISR, as explained in the main text, at $\sqrt{s} = 175$ GeV and $\sqrt{s} = 205$ GeV.
- Fig. 3** Total cross section as a function of y_{cut} in the JADE scheme for five-jet production via WW at $\sqrt{s} = 175$ GeV (continuous line), $\sqrt{s} = 190$ GeV (dashed line) and $\sqrt{s} = 205$ GeV (dotted line). The dot-dashed line in Fig. 3a gives the QCD contribution to five-jet production through point-like annihilation at $\sqrt{s} = 175$ GeV. In Fig. 3a ISR effects are not included. In Fig. 3b we compare results which include ISR effects with those without ISR, as explained in the main text, at $\sqrt{s} = 175$ GeV and $\sqrt{s} = 205$ GeV for the WW signal only.
- Fig. 4** Gluon spectra in six-jet production via WW at $\sqrt{s} = 175$ GeV. The continuous line gives the energy distribution for a single gluon, while the short-dashed line and the long-dash-short-dash line give the spectrum of the most and least energetic of the two gluons, respectively.
- Fig. 5** Integral over phase-space of the sum of the interference between the diagrams in set A1 with those in set A2 and of the diagrams in set A3 with those in set A4 at $\sqrt{s} = 175$ GeV.



(A1)

(A2)



(A3)

(A4)

Fig. 1

6 jet distribution

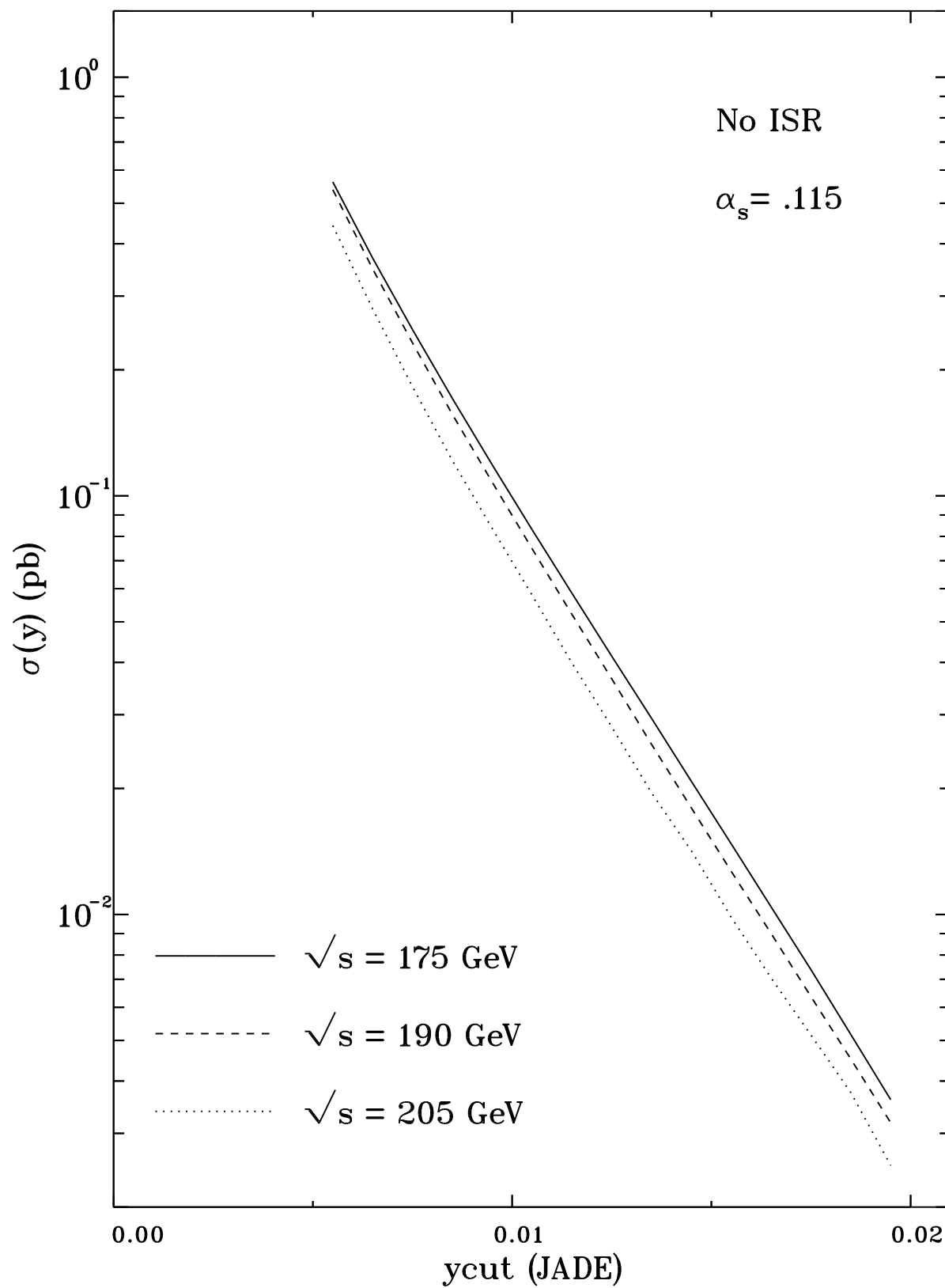


Fig. 2a

6 jet distribution

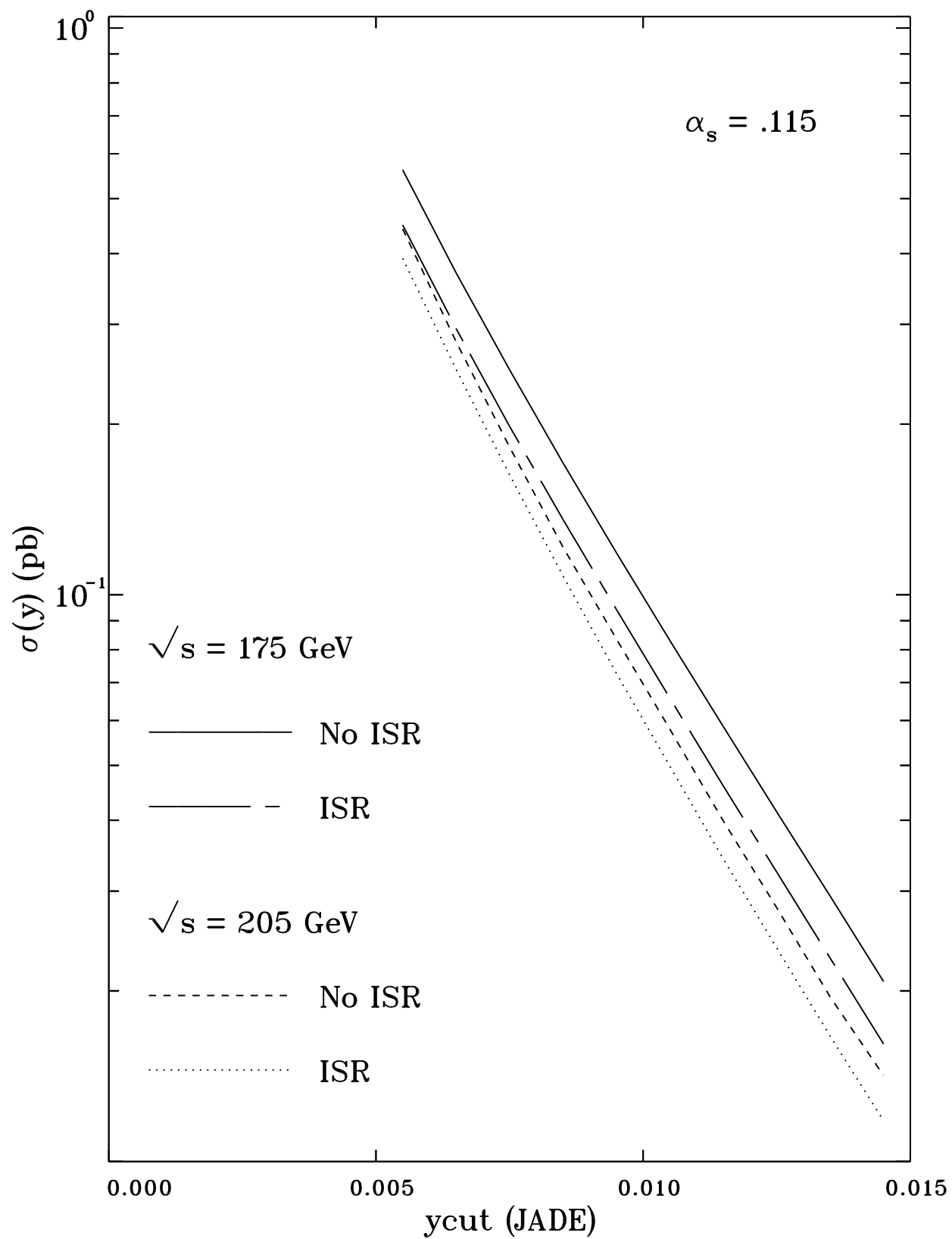


Fig. 2b

5 jet distribution

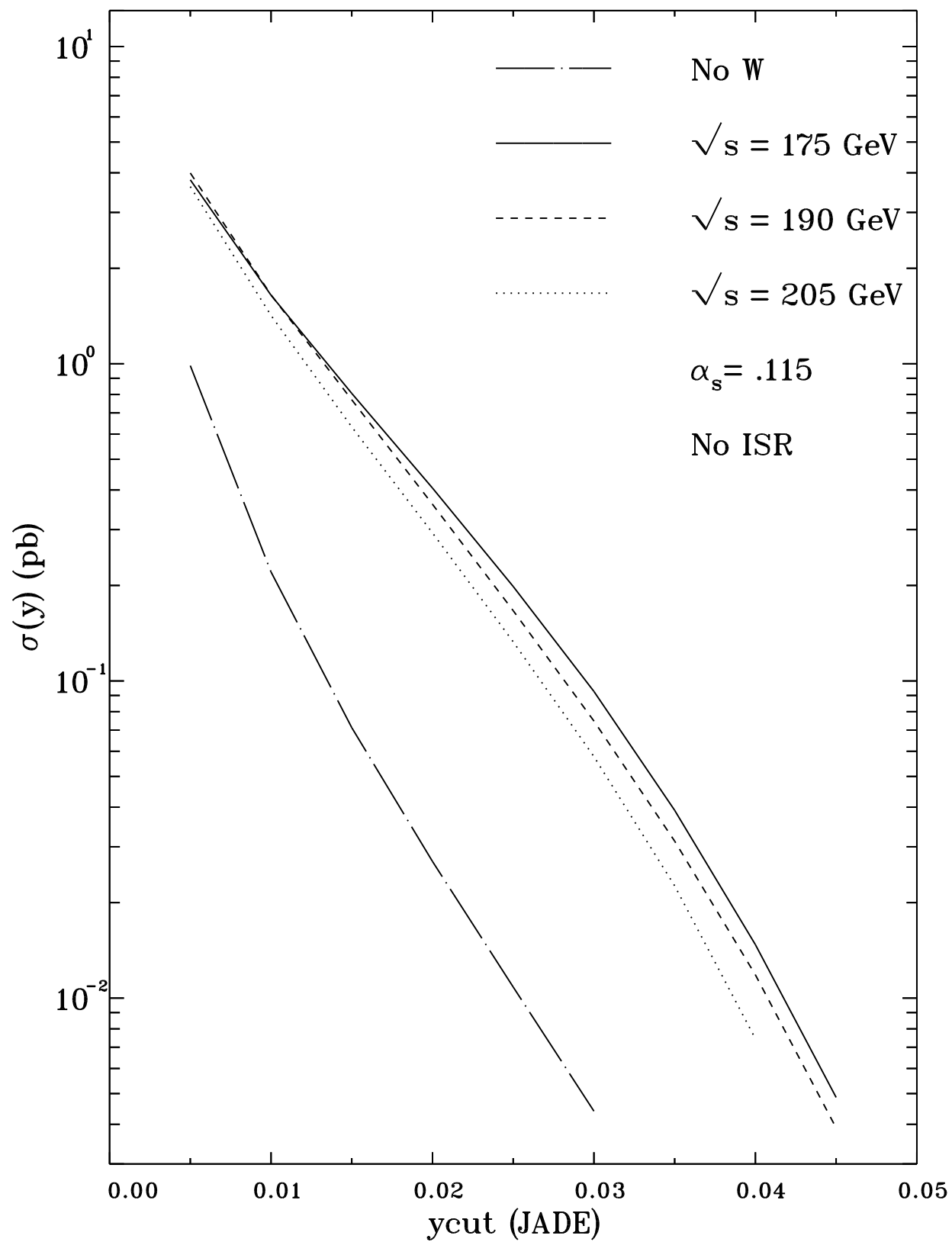


Fig. 3a

5 jet distribution

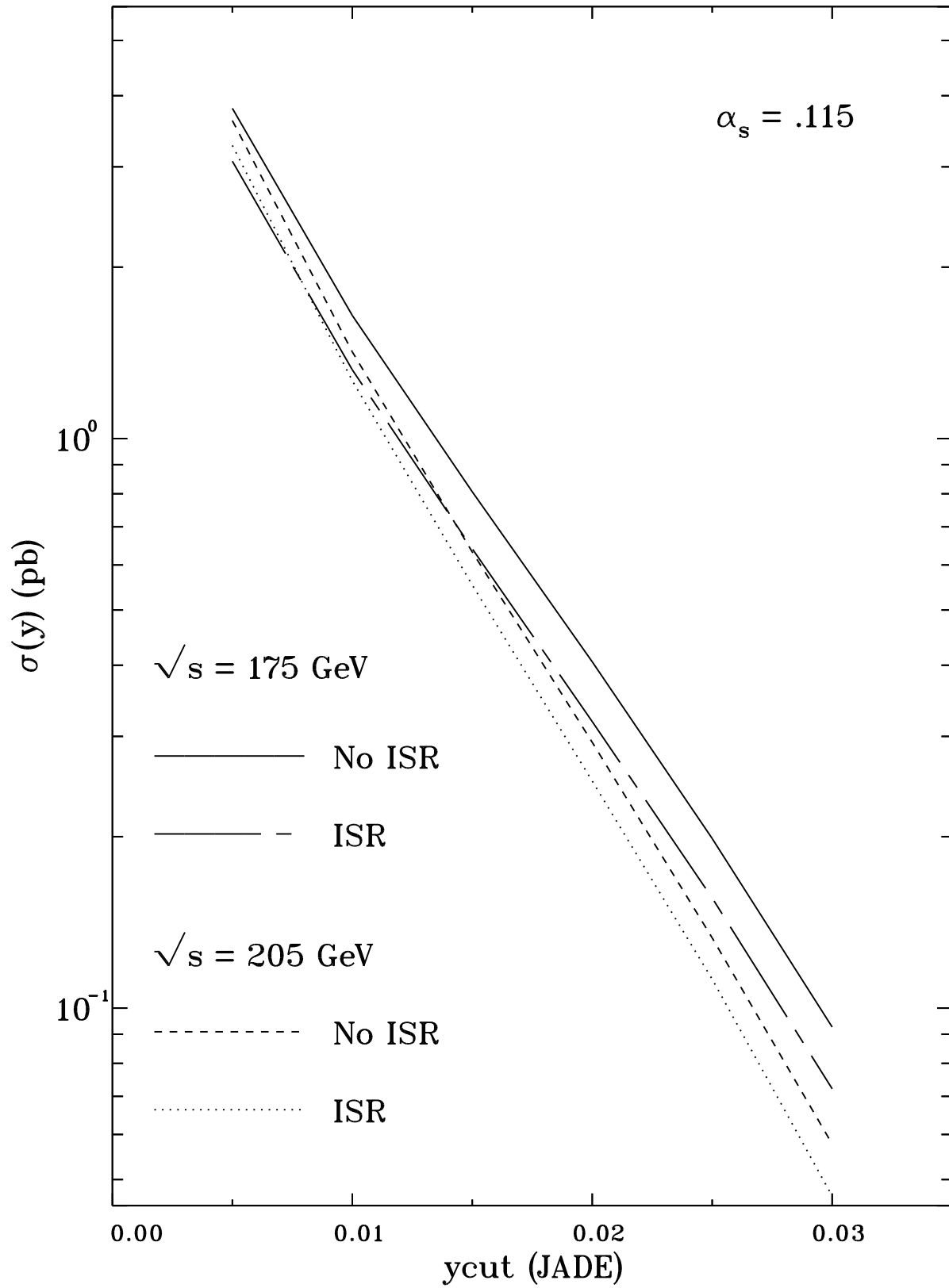


Fig. 3b

6 jet: Gluon energy distribution

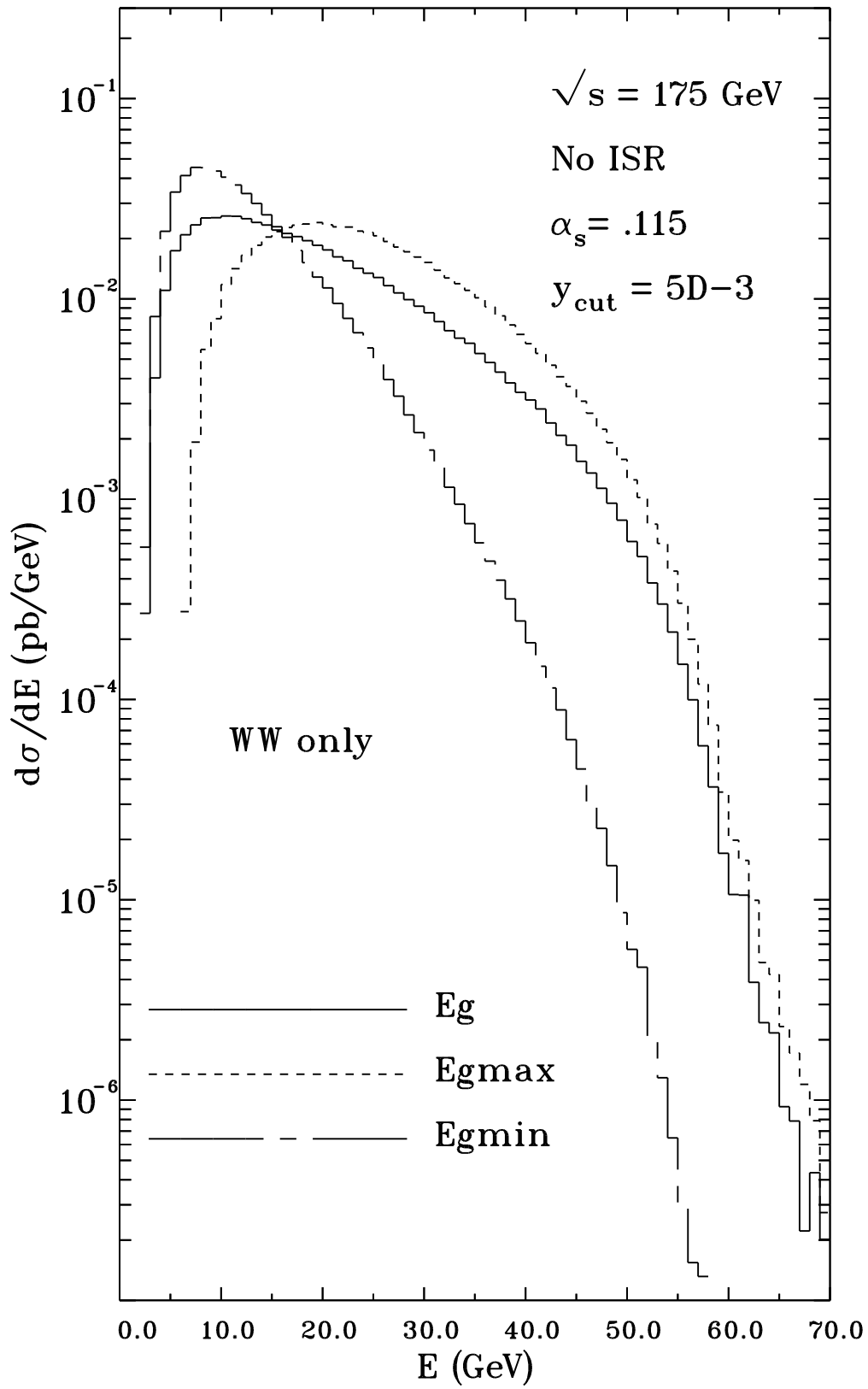


Fig. 4

6 jet interference

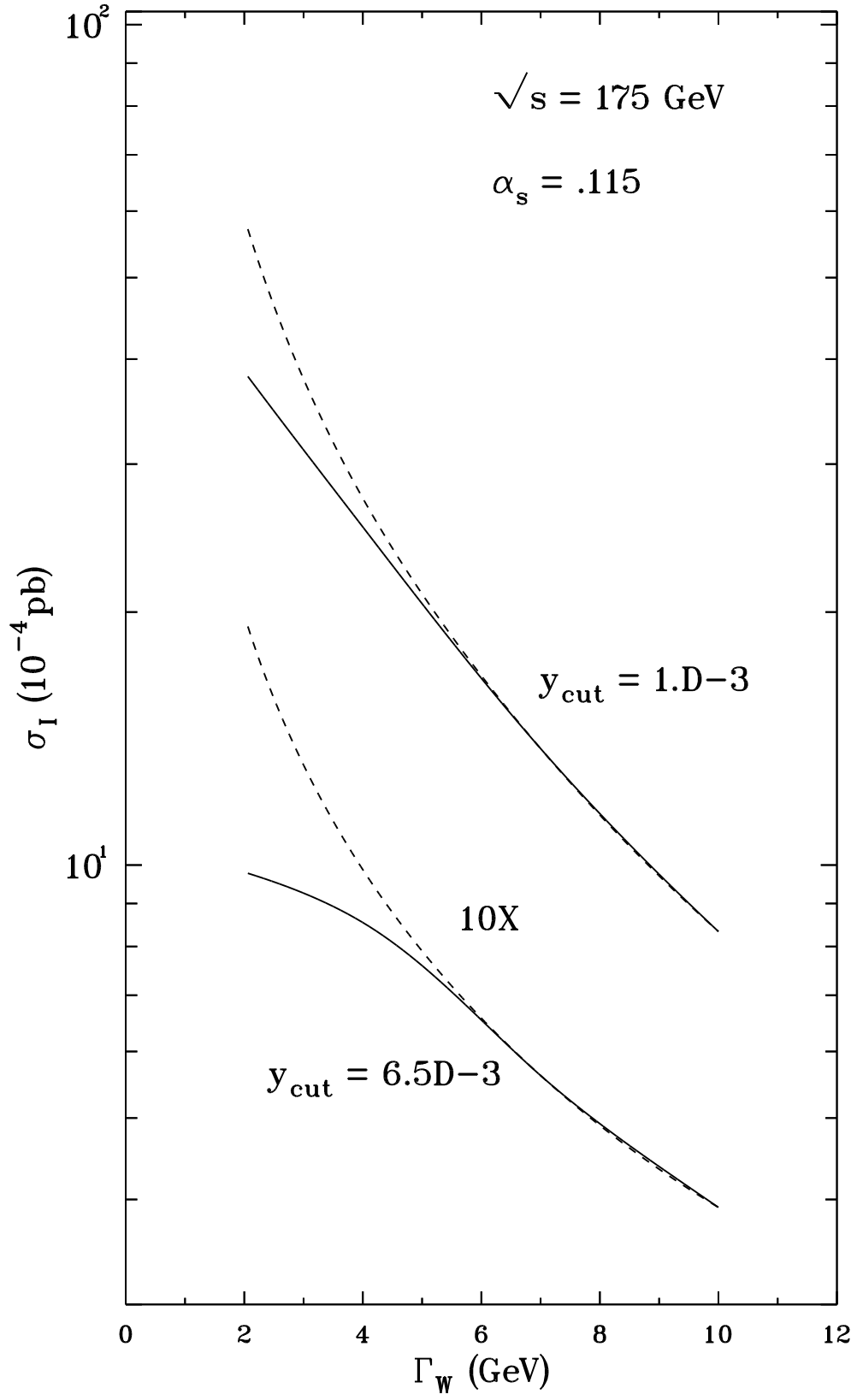


Fig. 5